ACS APPLIED MATERIALS & INTERFACES

Letter

www.acsami.org

Air-Pressure Tunable Depletion Width, Rectification Behavior, and Charge Conduction in Oxide Nanotubes

Yahya Alivov,*[,†] Hans H. Funke,[†] Vivek Singh,[†] and Prashant Nagpal*[,†,‡,§]

[†]Department of Chemical and Biological Engineering, [‡]Materials Science and Engineering, and [§]Renewable and Sustainable Energy Institute, University of Colorado, Boulder, Colorado, United States

Supporting Information

ABSTRACT: Metal-oxide nanotubes provide large surface areas and functionalizable surfaces for a variety of optical and electronic applications. Here we report air-tunable rectifying behavior, depletion width modulation, and two-dimensional (2D) charge conduction in hollow titanium-dioxide nanotubes. The metal contact forms a Schottky-diode in the nanotubes, and the rectification factor (on/off ratio) can be varied by more than 3 orders of magnitude ($1-2 \times 10^3$) as the air pressure is increased from 2 mTorr to atmospheric pressure. This behavior is explained using a change in depletion width of these thin nanotubes by adsorption of water vapor on both surfaces of a hollow nanotube, and the resulting formation of a metal−insulator−semiconductor (MIS) junction, which controls the 2D charge conduction properties in thin oxide nanotubes.

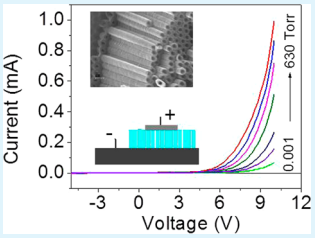

KEYWORDS: *metal-oxide nanotubes, Schottky diode, air-tunable rectification, air-gating, chemical diodes*

Quasi-one-dimensional hollow semiconductor nanostructures like nanotubes and nanowires provide large surface areas and functionalized surface for applications in a variety of optical and electronic devices.[1−4] Reduced dimensions and large surface area-to-volume ratios can have a significant impact on the electronic properties of these semiconductor nanostructures and conventional metal−semiconductor theory cannot adequately describe their properties.[5] The nanostructure surfaces can affect the charge conduction mechanism and other electronic properties, compared to their bulk counterparts.[6−11] However, the large surface areas in these nanostructures have not been utilized to tune the electronic properties of these semiconductors, and study novel physical properties as a result of the tailored surface interactions. Here, we report an air-tunable rectifying Schottky diode using a metal contact with titanium-dioxide nanotubes (TiO_2 NTs), with rectification factor (on/off ratio) tunable from 1 to 1×10^3 by simply changing the air pressure. We also show that this three-orders-of-magnitude change in rectifying behavior occurs because of the tunability of the depletion widths in these thin oxide nanotubes by adsorption of water vapor, and interesting transitions in charge transport behavior can be observed from space charge-limited conduction, at low voltages, to superlinear 2D charge conduction in thin nanotubes, at higher applied bias. Similar surface tunability and "chemical-gating" behavior can also be expected in other quasi-one-dimensional nanostructures, opening up the possibility of developing functional devices or studying interesting 2D charge conduction properties in semiconductor nanotubes.

TiO_2 NTs were grown by anodization[6−9] in an electrolyte consisting of ethylene glycol+1%NH_4F+1%H_2O.[8,9] The length and diameter of the TiO_2 nanotubes were controlled by varying the growth time and the anodization voltage (scanning electron micrographs (SEM) shown in Figure 1a, Figure S1 in the Supporting Information). The anodization voltage was varied in the range 8−120 V resulting in nanotube diameters ranging from 20−322 nm. The length of the nanotubes was varied in the range 3−20 μm by varying growth time. Unless otherwise noted, all results presented below correspond to nanotubes with a diameter of ∼100 nm and a height of ∼10 μm. Scanning tunneling spectroscopy (STS) showed that all TiO_2 NTs demonstrated n-type conductivity (see Figure S1 in the Supporting Information) because of oxygen vacancies[2,8,10] present in the nominally undoped NTs. Using 100 nm diameter nanotubes, we characterized their electronic properties with "chemical gating" (using different gases) in an evacuated chamber with electrical feedthrough. We measured the current−voltage ($I-V$) characteristics of the nanotubes using anodized titanium metal foil as bottom contact and a metal electrode as the top contact for the nanotube film (Figure 1a, inset). Air humidity and temperature during measurements were ∼57% and 22 °C, respectively. By changing the air pressure (P) in the evacuated chamber from 2 mTorr to 630 Torr (ambient pressure in the lab), we observed that the current changed over several orders of magnitude, showing a strong decrease in resistivity of the nanotubes with increase in pressure ("air-gating", Figure 1b and Figure S2 in the Supporting Information). Moreover, because of the doped nature of the nanotubes (as seen in STS measurements, Figure S1 in the Supporting Information), we saw a strong diode response, where the ratio of forward to reverse bias ($I(V)/I(-V)$), or diode on/off ratio, changed significantly by changing

Received: November 3, 2014
Accepted: January 16, 2015
Published: January 16, 2015

DOI: 10.1021/am5076666
ACS Appl. Mater. Interfaces 2015, 7, 2153−2159

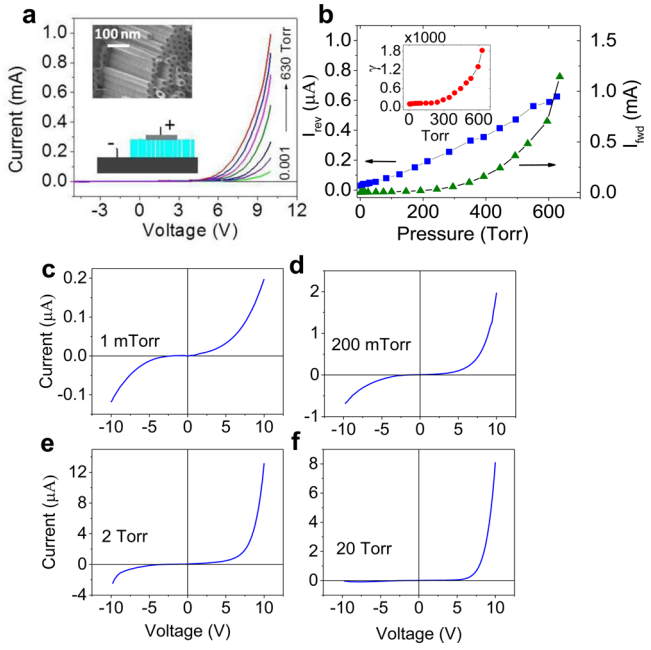

Figure 1. (a) Current–voltage characteristics of TiO_2 nanotubes in air ambient as a function of pressure. Inset shows SEM image of nanotubes. (b) Reverse current I_{fwd} (blue square), forward current I_{rev} (green triangle), and rectification factor γ (inset) as a function of pressure. Data extracted from Figure 1A. (c–f) I–V characteristics of TiO_2 nanotubes at low pressures (c) 1 mTorr when I–V is fully symmetric, and higher pressures (d) 200 mTorr (or 0.2 Torr), (e) 2 Torr, and (f) 20 Torr. Air humidity and temperature during measurements was 57% and 22 °C, respectively.

the air pressure. Although some changes in resistivity of large surface area nanostructures have been seen because of adsorption or desorption of gas molecules on the surface,[11−14] no rectifying behavior and its tuning with air pressure (tunable "chemical transistors" and "chemical diodes") have been reported yet. This air-gating behavior with large changes in resistivity and electronic properties (discussed below) with air-pressure resembles the field-effect transistor characteristics. Air-tunable nanotube diodes show a rectification factor γ ($\gamma = I(V)/I(-V)$) that increases superlinearly with air pressure P (Figure 1b, inset), with a "turn-on" pressure of ∼300 mTorr. At atmospheric pressure (630 Torr) the rectification factor γ was $\sim 2 \times 10^3$ (using $V = \pm 10$, Figure 1f) and it decreased with decrease in pressure, so that at 2 mTorr (0.002 Torr) I–V curves becomes almost symmetric with $\gamma \approx 1$ (Figure 1c). The transformation from symmetric to asymmetric behavior of I–V curves as pressure increases is shown in Figure 1b (inset). The change in the rectification factor of the chemical diode with pressure (from 0.002 to 20 Torr, Figure 1c–f) indicates possible changes in charge carrier concentrations, charge conduction properties, depletion width, and potentially the band alignment at the large interfaces in two-dimensional oxide nanotube surfaces. These I–V characteristics, rectification behavior, and its dependence on air pressure is highly reversible with variations of less than 10% across several measurements. This is seen from Figure S3 in the Supporting Information, which presents the rectification factors $\gamma = I(10\ V)/I(-10\ V)$ after the first and fifth runs (for clarity only first and fifth consecutive runs are shown). Because the effect of pressure on the I–V curves is completely reversible, the changes in transport properties are likely due to adsorption and desorption of molecules on these 2D interfaces.

To further understand the role of adsorption of molecule on the electronic properties of TiO_2 semiconductor nanotubes, we investigated the effect of individual components of air: nitrogen, oxygen, and water vapor, on charge transport in nanotubes to decouple the chemical nature of the observed interfacial phenomenon. The measurement chamber was first evacuated to a base pressure of 2 mTorr, and then pure gases were introduced at different pressures to evaluate their effect on the 2D charge transport (Figure 2). We found that nitrogen and

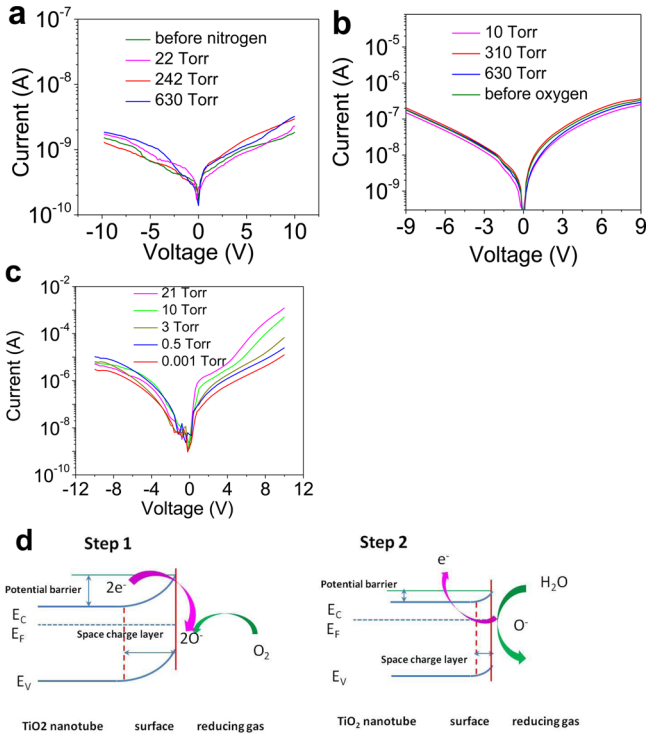

Figure 2. I–V characteristics in logarithmic scale for TiO_2 nanotubes in pure (a) nitrogen, (b) oxygen, and (c) water vapor atmosphere as a function of pressure. These gases were introduced after evacuating the chamber. Pure water vapor was introduced using liquid water in an evacuated chamber, as shown in Figure S4 in the Supporting Information. No effect of oxygen and nitrogen gas is observed on TiO_2 nanotube conductivity, whereas the effect of water vapor electrical properties is dramatic. (d) Schematic diagram of band bending and gas reaction of a TiO_2 nanotubes based sensor: (Step 1) before and (Step 2) after exposing to gas.

oxygen did not have any appreciable effect on the electrical properties of TiO_2 nanotubes, as shown in Figures 2a, b. However, water vapor (introduced using an evacuated chamber setup shown in Figure S4 in the Supporting Information) produced a profound impact on the resistivity and rectification behavior of chemical diodes (Figure 2c). Thus, water vapor (H_2O) partial pressure in air was likely responsible for the change of resistivity and rectifying behavior of TiO_2 nanotubes. Because water vapor was available in air, and no additional water was introduced into the chamber during the experiments, we refer to this phenomenon as an effect of "air pressure". The partial water vapor pressure corresponding to air humidity and temperature during measurements (∼57% and 22 °C, respectively) is around ∼11 mTorr (water vapor pressure at 22 °C is ∼21 Torr). The effect of water vapor was studied as a

DOI: 10.1021/am5076666
ACS Appl. Mater. Interfaces 2015, 7, 2153−2159

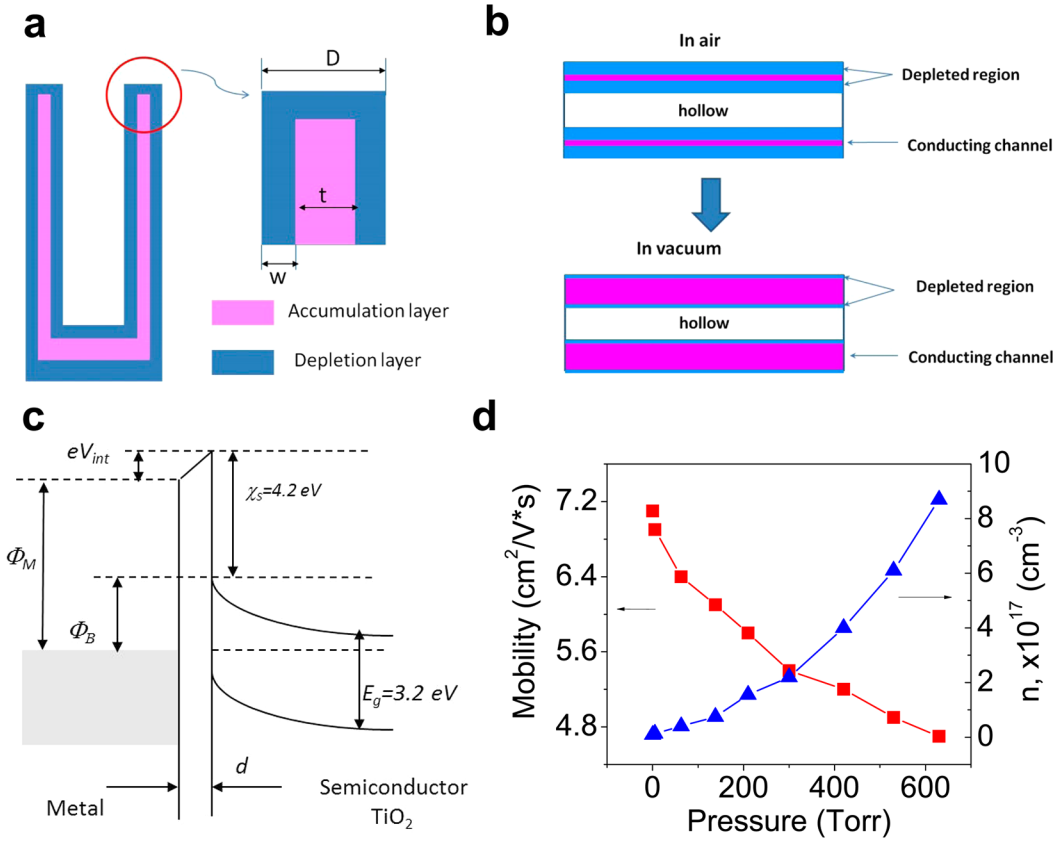

Figure 3. (a) Schematic of the MIS structure, to illustrate charge depletion on the nanotube surface and its dependence on pressure. (b) Schematic showing change in the depletion layer thickness in a TiO_2 nanotube upon exposure to air; the depletion layer thickness of the nanotube exposed to air at atmospheric pressure is smaller than that of the nanotube in vacuum. (c) Energy band diagram of MIS structure where d, E_g, eV_{int}, Φ_M, Φ_B, and χ_s stand for depleted region thickness, energy bandgap, band bending, metal work function, barrier height, and electron affinity, respectively. (d) Charge carrier concentration and mobility as a function of pressure measured in air ambient (air humidity 57%).

function of nanotube height and no notable dependence was observed within a nanotube height range of 3−20 μm.

The change in charge conduction for TiO_2 nanotubes, and the observed chemical rectification, is explained by a surface-depletion model.[4,15,16] In this model, the surface reaction between chemisorbed oxygen (oxygen vacancies) and reducing gases is responsible for the change in conductivity of the metal oxide nanotubes. When TiO_2 nanotubes are exposed to air, the adsorption of water vapor molecules on nanotube surface results in charge transfer from gas molecules to the nanotube via surface reaction on previously chemisorbed oxygen species,[4,16] thereby changing the charge carrier concentration and charge conduction properties of the nanotubes. Thus, the surface reaction of gases consists of two steps (Figure 2d). In the first step (Figure 2d, left) the oxygen is chemisorbed on the as-synthesized nanotube surface by capturing free electrons from the conduction band of TiO_2 and forming charged species O_2^-, O^-, and O^{2-} according to the reactions (eqs 1−4):[4,15,16]

$$O_2(g) \rightarrow O_2(ads) \quad (1)$$

$$O_2(ads) + e^- \rightarrow O_2^-(ads) \quad (2)$$

$$O_2^-(ads) + e^- \rightarrow 2O^-(ads) \quad (3)$$

$$O^-(ads) + e^- \rightarrow O^{2-}(ads) \quad (4)$$

where (g) refers to gas molecules and (ads) refers to adsorbed molecules. Therefore, as-grown TiO_2 nanotubes are nominally n-type because of these oxygen vacancies (V_O), which act as donors that supply electrons in the conduction band. Because the lower edge of the TiO_2 conduction band is higher than the chemical potential of O_2, 4.3 and 5.7 eV below the vacuum level, respectively,[4,7] electrons transfer from the conduction band of TiO_2 to the adsorbed oxygen atoms acting as electron traps. As a result of the diminishment of the charge carrier concentration near the surface region, a depletion region (space charge region) is created in the wall of the TiO_2 nanotube as shown in Figure 3a, b, leading to an increase in the electrical resistance of the TiO_2 layer.

In a second step (Figure 2d, right), when nanotubes are exposed to water vapor, water molecules react with the pre-existing adsorbed oxygen vacancies O_2^-, O^-, and O^{2-} at the TiO_2 nanotube surface or crystal lattice oxygen O to form OH hydroxyl groups. The precise mechanism of the water molecule reaction with chemisorbed oxygen ions is under debate and two possible mechanisms can be expressed by the following eqs 5 and 6[16]

$$H_2O + 2Ti_{Ti} + O_O \leftrightarrow (Ti_{Ti} - OH) + (OH)_O^+ + e^- \quad (5)$$

$$H_2O + 2Ti_{Ti} + O \leftrightarrow 2(Ti_{Ti} - OH) + V_O^{\cdot} + 2e^- \quad (6)$$

where (Ti_{Ti}^+−OH^-) presents an isolated hydroxyl or OH group and (OH_O^+) is the rooted one, i.e., OH groups including lattice oxygen. The first reaction (eq 5) implies the homolytic dissociation of water and the reaction of the neutral H atom

DOI: 10.1021/am5076666
ACS Appl. Mater. Interfaces 2015, 7, 2153−2159

with the TiO_2 crystal lattice oxygen. The built up rooted OH group gets ionized with the injection of an electron in the conduction band as it has a lower electron affinity. The second mechanism (eq 6) takes into account the possibility of the reaction between hydrogen atoms and the lattice oxygen (heterolytic dissociation) and the binding of the resulting hydroxyl group to the Ti atom. The resulting oxygen vacancy, which is a shallow donor, produces additional electrons.[16,17] These interactions lead to an increase in carrier concentration in the TiO_2 nanotube walls and a decrease in the surface depletion layer width as illustrated in Figure 3a, b, to a decrease in the electrical resistance of the TiO_2 nanotubes. On reducing the pressure in the chamber, this adsorption process is reversed, leading to the loss of these reversible dopants, and the $I-V$ returns to the symmetric undoped TiO_2 nanotube characteristics (Figure 1c). Therefore, the adsorbed oxygen molecules create a depletion region at the interface, which modifies the transport in the thin 2D nanotube channel (Figure 3a, b).

To further probe the charge conduction behavior in the chemical diodes, we calculated the carrier concentration of the nanotubes using $I-V$ curves in the intermediate bias regime, where the reverse-biased Schottky barrier dominates the total current[8,17,18,19]

$$\ln(I) = \ln(S) + e\left(\frac{1}{kT} - \frac{1}{E_0}\right)V + \ln I_s \quad (1)$$

where I is the current through the Schottky barrier, S is the contact area associated with this barrier, E_0 is a parameter depending on carrier concentration n, e is the electron charge, k is the Boltzmann constant, and I_s is a function of the applied bias. The slope of $\ln(I)$ vs V equals $e((1/kT) - (1/E_0))$, where$E_0 = E_{00}\coth(E_{00}/kT)$, and $E_{00} = (\hbar e/2)(n/m^*\varepsilon)^{1/2}$, h is the Planck's constant, ε_0 is the vacuum permittivity, $\varepsilon = 31\varepsilon_0$ is the dielectric constant for TiO_2, k is the Boltzmann constant, and $m^* = m_0$ is the electron effective mass. The slope of ln I vs. V equals $e((1/kT) - (1/E_0))$, and was used to calculate carrier (electron) concentration n using the expression for the E_{00} (see Figure S5 in the Supporting Information). Using n, the electron mobility (μ) is extracted using the relationship $\mu = 1/(ne\rho)$, where ρ is the resistivity of the nanotubes. The resistivity, ρ, of individual nanotubes was calculated using resistance $R = \Delta V/\Delta I$, and $R = L\rho/S$, where L is the length of nanotubes and S is the contact area of the tip. We studied the charge carrier concentration and mobility as a function of vapor pressure (Figure 3d), to understand the charge transport mechanism. The carrier concentration n was found to be 9.2×10^{15} cm^{-3} at the lowest pressure 2 mTorr, and increased with an increase in pressure, reaching 8.7×10^{17} cm^{-3} at an atmospheric pressure of 630 Torr. While the carrier concentration was strongly influenced (by 2 orders of magnitude) by the chemical doping from adsorbed molecules, the carrier mobility showed a modest decrease, changing from 7.1 $cm^2/(V\ s)$ at 2 mTorr to 4.7 $cm^2/(V\ s)$ at 630 Torr.

To gain further insights into the Schottky junction formed between the metal contact and semiconductor TiO_2 nanotubes, we measured the barrier height for charge conduction, in ambient conditions (Ti sheet as the bottom contact and a metallic probe as top contact, Figure 1a inset). Using temperature-dependent $I-V$ characteristics of TiO_2 nanotubes, the slope of a Richardson plot ($\ln(I/T^2)$ vs $1/kT$) was used to calculate the Schottky barrier height (E_{SBH}) as 0.56 eV (Figure 4a). It was found that the measured barrier height E_{SBH} was

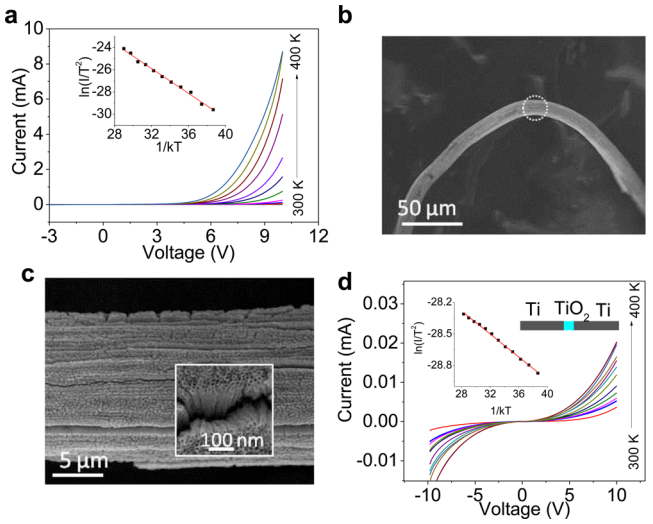

Figure 4. (a) Temperature-dependent I–V characteristics for TiO_2 nanotubes with a top metal contact (see Figure 1a, inset) in the temperature range of 300 K–400 K; (Inset) corresponding Richardson plot with corresponding linear fit. The extracted Schottky barrier height was 0.56 eV. (b) SEM image of the TiO_2 nanotube wire prepared by anodization of Ti wire of 20 μm diameter wire; (c) shows the magnified region circled in the image (b) to indicate the nanotube structure in the wire; inset shows further magnification to emphasize nanotubular structure. (d) Temperature dependent I–V characteristics for the Ti–TiO_2–Ti structure. The inset shows the Richardson plot with the corresponding linear fit. The extracted Schottky barrier height was 0.043 eV. These measurements were performed in ambient air (humidity 57%).

insensitive to the type of metal on top of the TiO_2 nanotube film. This indicates that the Fermi-level, which dictates the Schottky barrier, was pinned inside the semiconductor band gap on the nanotube surface. To understand the origin of this Fermi-level pinning, we performed experiments with identical contacts on both sides of the nanotubes. This was achieved by anodizing a part of the Ti wire, 20 μm in diameter, and using the non-anodized wire on either side as identical metal contacts (Figure 4b, and Figure S6–S8 in the Supporting Information; detailed methods are described in Supporting Information). The grown TiO_2 nanotubes were sandwiched between two identical Ti contacts (Figure 4b). The $I-V-T$ characteristics of this Ti–TiO_2–Ti structure and the corresponding Richardson plot revealed a much lower Schottky barrier height of 0.043 eV (Figure 4c). Therefore, the origin of Fermi-level pinning, band-bending and the large Schottky barrier height, and the novel chemical diode and chemical rectification can be well explained using a metal–insulator–semiconductor (MIS) junction in our model, where the insulating layer is the depleted nanotube surface layer (Figure 3b, c). The reversible chemical doping, using adsorption of vapor molecules, changes the thickness of the depletion layer with air pressure. As a result, the width of the depletion layer changes with air pressure and may extend from zero (accumulation) to half of the nanotube wall thickness. Because depletion layers grow from both sides of the nanotube wall at the air–nanotube interface (Figure 3a, b), the accumulation layer is strongly confined between the two depleted insulating layers. Although the thickness of the nanotube wall is ~10–15 nm, depending on air pressure, the width of the accumulation layer may be a few nanometers, leading to the formation of a 2D charge conduction, as illustrated in Figure 3b,c.

DOI: 10.1021/am5076666
ACS Appl. Mater. Interfaces 2015, 7, 2153–2159

Our model and chemical tuning of 2D charge conduction in thin depleted TiO_2 nanotubes was supported by several measurements. First, as the thickness (w) of depletion layer increases with a decrease in pressure, the tunneling probability for charge conduction exponentially decreases with w, proportional to $\sim \exp(-w)$.[20,21] The opposite trend is observed when the air-pressure is increased, the depletion layer thickness decreases as a result of the reaction with water molecules and the electron tunneling probability rapidly increases (Figures 1 and 3). Second evidence for our model comes from the nearly linear dependence of reverse current with air pressure, as shown in Figure 1b. Because the conductance ($G = I/V$) is linear with the depletion layer thickness d, $G \approx 2\sigma R_o d/h$ (Figure 5a), and

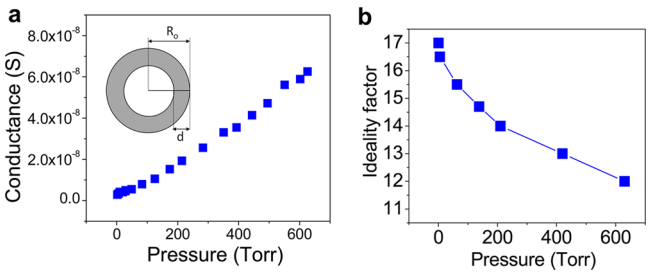

Figure 5. (a) Conductance of nanotubes as a function of ambient pressure demonstrating linear dependence. (b) Ideality factor of MIS Schottky diode as a function of ambient pressure.

the depletion width d is linear with air pressure P, the linear relationship between reverse current and air pressure (Figure 1b) can be explained using our model (Figure 5a). At reverse bias using Ohm's law $I=V/R$, it can be shown that the conductance G is in a linear relationship with the active region width d. The conductance G is equal to $G = 1/R = \sigma S/h$, where S is the cross-section area of the nanotube depletion region, h is the height of the nanotubes, and σ is the conductivity of the channel. Using the geometry of the nanotube, the cross-section S can be calculated: $S = R^2 - (R - d)^2 = 2R_o d - d^2$ (Figure 5a). For $d \ll R_o$ in our experiments, with a nanotube diameter 100 nm and a wall thickness of 10 nm, the second term d^2 can be neglected and the cross-section S is approximated to $S \approx 2R_o d$. Substituting S, we get the conductance $G \approx 2\sigma R_o d/h$ that shows a linear relationship with the depletion width d (Figure 5a). The third confirmation of the model comes from the dependence of the diode ideality factor on air pressure. The ideality factor n of the diode was estimated using equation[22]

$$n = \frac{q}{kT}\frac{dV}{d\ln I} \quad (2)$$

The ideality factor was 12 at atmospheric pressure and increases with a decrease of pressure, reaching 17 at 0.002 Torr, as shown in Figure 5b. The high value of the ideality factor is explained by the thickness of the insulation layer between the metal and semiconductor: The thicker the insulation layer, the higher the ideality factor.[11,22,23] Using the MIS structure in our model, the increase in ideality factor with pressure occurs because of the increase in thickness of the insulation layer at lower pressures.

Change in thickness of the depletion layer results in a change in charge transport mechanism, and strong confinement of charge conduction between depleted layers in TiO_2 nanotubes. The shape of the $I-V$ curves at different air pressures changes, showing two different slopes for strongly confined accumulation layers (Figure 6b). At low pressures, usually below 3 Torr, the $I-V$ curve exhibited only one slope, as shown in

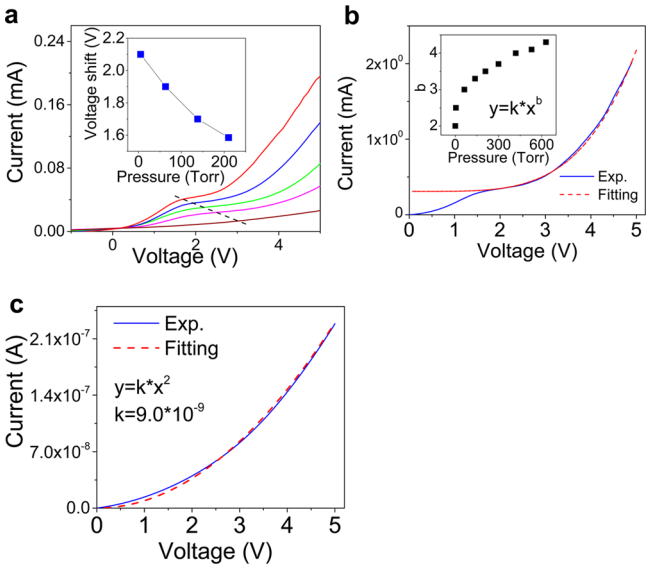

Figure 6. (a) $I-V$ characteristics of TiO_2 nanotubes measured in ambient air (humidity 57%) at different pressures to emphasize two slopes ("S-shape") at higher pressures; dashed line guides transition from one slope to the other. Inset shows inflection points (transition voltage V_t) as a function of pressure. (b) $I-V$ characteristics and fitting curve for nanotubes at 0.3 Torr pressure, showing square-dependence characteristic of space-charge limited conduction. (c) $I-V$ characteristics of charge conduction in the accumulation layer (second slope). (Inset) The extracted slope (b) as a function of air pressure reveals strongly confined 2D charge conduction.

Figure 6b, whereas at higher pressures (>3 Torr) a second slope appeared, as shown in Figure 6a, c. The transition voltage V_t between the first and second slopes depended on the air pressure, and shifted to lower values as the pressure increases ($V_t \approx 2.5$ V at 3 Torr shifted to lower values reaching 1.7 V at atmospheric pressure, Figure 6a, inset). This observation can be explained using 2D charge conduction. At low voltages, the transport is limited to the top depleted barrier layer; as the applied bias increases, the depletion layer breaks down and conduction occurs across the accumulation layer, leading to a drastic increase in current. The greater the thickness of the insulation layer, the higher the transition voltage V_t. The onset of the conduction through the accumulation layer is seen by the marked increase in current and the appearance of a second slope. The slopes of $I-V$ curves were fitted using the function $y = kx^b$. We found that the first slope had a power factor b very close to 2, and it did not change with pressure, whereas the second slope increases from 2 to 4.3 as the pressure increases from 3 to 630 Torr (Figure 6c, inset). Because electron conduction in nanotubes is strongly confined between two insulation layers (depleted layers) from both sides of the wall, the second slope in the $I-V$ curves can be explained by 2D charge conduction in the channel.[24] This is supported by the shift of V_t to lower values at higher pressures (because the depletion layer thickness is decreased), and the increase of the power factor b of the second slope with pressure (because 2D charge conduction becomes more pronounced as the pressure increases and hence the carrier concentration increases).

This explanation is further supported by the dependence of the electron transport properties on nanotube diameter.

DOI: 10.1021/am5076666
ACS Appl. Mater. Interfaces 2015, 7, 2153−2159

Different diameter TiO_2 nanotubes were grown from 20−320 nm (SEM images in Figure 7a−f) by adjusting the anodization voltage. Calculating the carrier concentration and mobility of the nanotubes as a function of diameter, we found that both increase with an increase in diameter, (from 2.3 to 7.8 $cm^2/(V\,s)$, and 0.2 to 1.7 × 10^{18} cm^{-3}, Figure 7g). The increase in mobility can also be explained by our model and 2D charge conduction in TiO_2 nanotubes as the diameter increases.

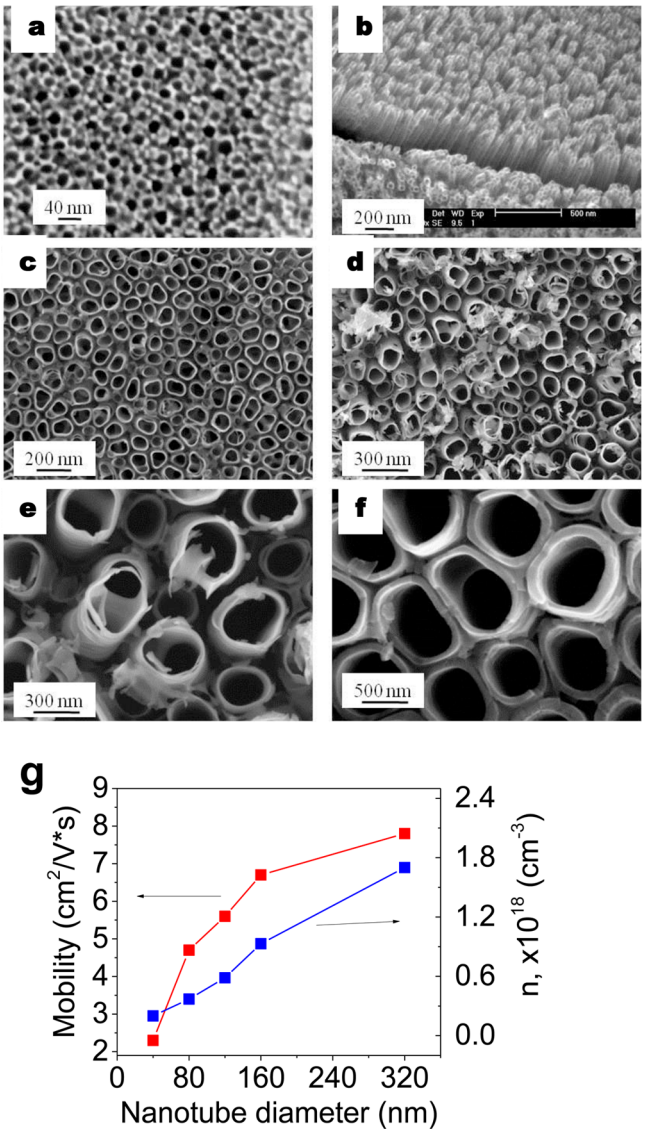

Figure 7. (a−f) SEM images of the TiO_2 nanotubes with different diameters grown at different anodization: a, b c, d, e, and f correspond to nanotubes with diameters 20, 43 (grown at 15 V), 86 (30 V), 170 (60 V), and 322 nm (120 V).(g) Mobility (red) and carrier concentration (blue) as a function of nanotube diameter; the measurements were performed in air ambient (humidity 57%).

In conclusion, we have shown an air-tunable rectifying behavior in TiO_2 semiconductor nanotubes. This chemical diode effect is explained by formation of a Schottky-diode in the nanotubes (with the metal contact), and the rectification factor of the diodes (on/off ratio) can be varied by 3 orders of magnitude (1−2 × 10^3) as the air pressure is increased from 2 milliTorr to atmospheric pressure. This behavior was using explained a metal−insulator-semiconductor (MIS) junction in our model, and the change in depletion width (insulator) in thin nanotubes by adsorption of water vapor. This phenomenon was also used to control the 2D charge conduction properties in thin oxide nanotubes. These results provides new insights, and can enable many new applications using the rectification behavior with air (water vapor) pressure for new types of devices such as "chemical diodes", "chemical transistors", pressure sensors, and altitude meters.

■ ASSOCIATED CONTENT

Supporting Information

Detailed methods, characterization, and Figures S1−S8. This material is available free of charge via the Internet at http://pubs.acs.org.

■ AUTHOR INFORMATION

Corresponding Authors

*E-mail: yahya.alivov@oxinst.com.
*E-mail: pnagpal@colorado.edu.

Notes

The authors declare no competing financial interest.

■ ACKNOWLEDGMENTS

The authors acknowledge financial support for this work by National Science Foundation NSF CAREER Award CBET-1351281.

■ REFERENCES

(1) Ohno, Y.; Young, D.; Beschoten, B.; Matsukura, F.; Ohno, H.; Awschalom, D. Electrical Spin Injection in a Ferromagnetic Semiconductor Heterostructure. *Nature* **1999**, *402*, 790−792.
(2) Oregan, B.; Gratzel, M. A Low-Cost, High-Efficiency Solar Cell Based on Dye-Sensitized Colloidal TiO_2 Films. *Nature* **1991**, *353*, 737−740.
(3) Chen, X.; Wong, C.; Yuan, C.; Zhang, G. Nanowire-Based Gas Sensors. *Sens. Actuators, B* **2013**, *177*, 178−195.
(4) Kolmakov, A.; Moskovits, M. Chemical Sensing and Catalysis by One-Dimensional Metal-Oxide Nanostructures. *Annu. Rev. of Mater. Res.* **2004**, *34*, 151−180.
(5) Leonard, F.; Talin, A. A. Size-Dependent Effects on Electrical Contacts to Nanotubes and Nanowires. *Phys. Rev. Lett.* **2006**, *97*, 026804.
(6) Gong, D.; Grimes, C. A.; Varghese, O. K.; Hu, W. C.; Singh, R. S.; Chen, Z.; Dickey, E. C. Titanium Oxide Nanotube Arrays Prepared by Anodic Oxidation. *J. Mater. Res.* **2001**, *16*, 3331−3334.
(7) Nah, Y. C.; Paramasivam, I.; Schmuki, P. Doped TiO_2 and TiO_2 Nanotubes: Synthesis and Applications. *ChemPhysChem* **2010**, *11*, 2698−2713.
(8) Alivov, Y.; Singh, V.; Ding, Y.; Cerkovnik, L.; Nagpal, P. Doping of Wide-Bandgap Titanium-Dioxide Nanotubes: Optical, Electronic and Magnetic Properties. *Nanoscale* **2014**, *6*, 10839−1049.
(9) Alivov, Y.; Singh, V.; Ding, Y.; Nagpal, P. Transparent Conducting Oxide Nanotubes. *Nanotechnology* **2014**, *25*, 385202.
(10) Linsebigler, A. L.; Lu, G. Q.; Yates, J. T. Photocatalysis on TiO2 Surfaces: Principles, Mechanisms, and Selected Results. *Chem. Rev.* **1995**, *95*, 735−758.
(11) Harnack, O.; Pacholski, C.; Weller, H.; Yasuda, A.; Wessels, J. M. Rectifying Behavior of Electrically Aligned ZnO Nanorods. *Nano Lett.* **2003**, *3*, 1097−1101.
(12) Hernandez-Ramirez, F.; Tarancon, A.; Casals, O.; Rodriguez, J.; Romano-Rodriguez, A.; Morante, J. R.; Barth, S.; Mathur, S.; Choi, T. Y.; Poulikakos, D.; Callegari, V.; Nellen, P. M. Fabrication and Electrical Characterization of Circuits Based on Individual Tin Oxide Nanowires. *Nanotechnology* **2006**, *17*, 5577−5583.
(13) Hernandez-Ramirez, F.; Tarancon, A.; Casals, O.; Pellicer, E.; Rodriguez, J.; Romano-Rodriguez, A.; Morante, J. R.; Barth, S.;

DOI: 10.1021/am5076666
ACS Appl. Mater. Interfaces 2015, 7, 2153−2159

Mathur, S. Electrical Properties of Individual Tin Oxide Nanowires Contacted to Platinum Electrodes. *Phys. Rev. B* **2007**, *76*, 085429.
(14) Leonard, F.; Talin, A. A.; Swartzentruber, B. S.; Picraux, S. T. Diameter-Dependent Electronic Transport Properties of Au-catalyst/Ge-Nanowire Schottky Diodes. *Phys. Rev. Lett.* **2009**, *102*, 106805.
(15) Penner, R. M. Chemical Sensing With Nanowires. *Annu. Rev. Anal. Chem.* **2012**, *55*, 461−485.
(16) Barsan, N.; Weimar, U. Conduction Model of Metal Oxide Gas Sensors. *J. Electroceram.* **2001**, *7*, 143−167.
(17) Singh, V.; Beltran, I. J. C.; Ribot, J. C.; Nagpal, P. Photocatalysis Deconstructed: Design of a New Selective Catalyst for Artificial Photosynthesis. *Nano Lett.* **2014**, *14*, 597−603.
(18) Zhang, Z. Y.; Jin, C. H.; Liang, X. L.; Chen, Q.; Peng, L. M. Current-Voltage Characteristics and Parameter Retrieval of Semiconducting Nanowires. *Appl. Phys. Lett.* **2006**, *89*, 073102.
(19) Bai, X. D.; Golberg, D.; Bando, Y.; Zhi, C. Y.; Tang, C. C.; Mitome, M.; Kurashima, K. Deformation-Driven Electrical Transport of Individual Boron Nitride Nanotubes. *Nano Lett.* **2007**, *7*, 632−637.
(20) Hattori, K.; Izumi, Y. The Electrical Characteristics of Degenerate InP Schottky Diodes with an Interfacial Layer. *J. Appl. Phys.* **1982**, *53*, 6906−6910.
(21) Card, H. C.; Rhoderic, E. H. Studies of Tunnel MOS Diodes I. Interface Effects in Silicon Schottky Diodes. *J. Phys. D:Appl. Phys.* **1971**, *4*, 1589−1601.
(22) Sze. S. M. *Physics of Semiconductor Devices*, 3rd ed.; Wiley: New York, 2007.
(23) Kim, J. R.; Oh, H.; So, H. M.; Kim, J. J.; Kim, J.; Lee, C. J.; Lyu, S. C. Schottky Diodes Based on a Single GaN Nanowire. *Nanotechnology* **2002**, *13*, 701−704.
(24) Pandey, S.; Fraboni, B.; Cavalcoli, D.; Minj, A.; Cavallini, A. Two-Dimensional Electron Gas Properties by Current-Voltage Analyses of $Al_{0.86}In_{0.14}N$/AlN/GaN Heterostructures. *Appl. Phys. Lett.* **2011**, *99*, 012111.

DOI: 10.1021/am5076666
ACS Appl. Mater. Interfaces 2015, 7, 2153−2159